Sensors & Transducers Journal, Vol.0, Issue 0, Month 2009, pp.

www.sensorsportal.com

Sensors & Transducers

ISSN 1726-5479

http://www.sensorsportal.com

A Multiscale Model of Cantilever Arrays and its Validation and Identification

Michel LENCZNER, Emmanuel PILLET, Scott COGAN and Hui HUI

FEMTO-ST, 26 Chemin de l'épitaphe, 25000 Besançon, France

Phone: +33 03 81 83 26 69, Fax : +33 (0)3 81 85 39 98,

E-mail : michel.lenczner@utbm.fr, manu.pillet@gmail.com, scott.cogan@univ-fcomte.fr, hui.hui@femto-st.fr

Received: */Accepted:* */Published:*

Abstract: We present a simplified model of mechanical behavior of large cantilever arrays with discoupled rows in the dynamic operating regime. Since the supporting bases are assumed to be elastic, cross-talk effect between cantilevers is taken into account. The mathematical derivation combines a thin plate asymptotic theory and the two-scale approximation theory, devoted to strongly heterogeneous periodic systems. The model is not standard, so we present some of its features. We explain how each eigenmode is decomposed into a product of a base mode with a cantilever mode. We explain the method used for its discretization, and report results of its numerical validation with full three-dimensional Finite Element simulations. Finally, we provide a short description of parameter updating and identification techniques developed for the model.

Keywords: Cantilever Arrays, Multiscale Modeling, Homogenization, Strongly Heterogeneous Homogenization

1. Introduction

Cantilever arrays are used in a variety of application including Atomic Force Microscope arrays, for instance the Millipede from IBM dedicated to data storage, see in [1]. Modeling of large cantilever arrays is little developed. However, their direct numerical simulation, based on classical methods like Finite Element Methods, is prohibitive for today's computers, at least in a time compatible with designer time scale. The B. Bamieh's group has published a cantilever array model, see [2] among other papers. It takes into account electrostatic coupling, and its derivation is phenomenological. One of the authors has published a model for an elastic AFM Array in the static regime [3] and preliminary results for the dynamic regime [4].

2. Geometry of the problem

We consider a two-dimensional array of cantilevers, see Figure 1(a) for a two-dimensional view. It is comprised of rectangle parallelepiped bases crossing the array in which rectangle parallelepiped cantilevers are clamped. Bases are supposed to be connected in the x_1-direction only, so that the system behaves as a set of discoupled rows. Each of them is clamped at its ends. Concerning the unclamped end of cantilevers, we report two cases, one for free ends and one for ends equipped with rigid tips, as in Atomic Force Microscopes. The whole array is a periodic repetition of a same cell, in the two directions x_1 and x_2. We suppose that the number of columns and of rows of the array are sufficiently large, namely larger or equal to 10. Then, we introduce the small parameter ε^* equals to the inverse $1/N$ of the number of cantilevers in a row. We underline the fact that the technique presented in the rest of the paper can be extended to other geometries of cantilever arrays and even to other classes of microsystem arrays.

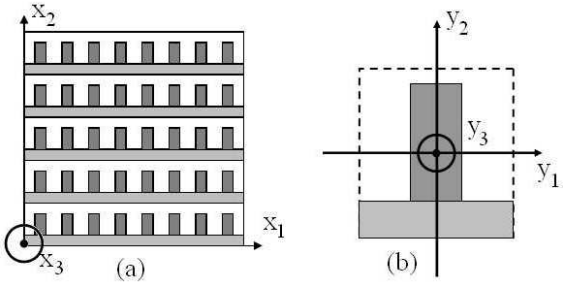

Fig. 1. Two-dimensional view of (a) the full cantilever array (b) a unit cell

3. Two-scale approximation

Each point of the three-dimensional space, with coordinates $x = (x_1, x_2, x_3)$, is decomposed as $x = x^c + \epsilon y$, where x^c represents the coordinates of the center of the cell to which x belongs, $\epsilon = \begin{pmatrix} \varepsilon^* & 0 & 0 \\ 0 & \varepsilon^* & 0 \\ 0 & 0 & 1 \end{pmatrix}$, and $y = \epsilon^{-1}(x - x^c)$ is the expanded relative position of x with respect to x^c. Points with coordinates y vary in the so-called *reference cell,* see the two-dimensional view on Fig. 1(b), that is obtained through a translation and the dilation ϵ^{-1} of any current cell in the array.

We consider the distributed field $u(x)$, of elastic deflections in the array, and we introduce its *two-scale transform,*

$$\widehat{u}^{\varepsilon}(\widetilde{x}, y) = u(x^c + \epsilon y),$$

for any $x = x^c + \epsilon y$ and $\widetilde{x} = (x_1, x_2)$. By construction, the two-scale transform is constant, with respect to its first variable $\widetilde{x}$, over each cell. Since it depends on the ratio ε^*, then it may be approximated by the asymptotic field, denoted by u^0, obtained for large number of cells (in both x_1 and x_2-directions) or equivalently when ε^* approaches (mathematically) 0:

$$\widehat{u}^{\varepsilon} = u^0 + O(\varepsilon^*)$$

where $O(\varepsilon^*)$ tends to zero when ε^* vanishes. The approximation u^0 is called the *two-scale approximation* of u. We mention that, as a consequence of the asymptotic process, the partial function $\widetilde{x} \mapsto u^0(\widetilde{x}, .)$ may be continuous instead of being piecewise constant.

Now, we consider that the field of elastic deflections u is a solution of the Love-Kirchhoff thin elastic plate equation in the whole mechanical structure, including bases and cantilevers. Furthermore, we assume that the ratio of cantilever thickness h_C to base thickness h_B is very small, namely

$$\frac{h_C}{h_B} \approx \varepsilon^{*4/3}. \tag{1}$$

This assumption is formulated so that the ratio of cantilever stiffness to base stiffness be very small, namely of the order of ε^{*4}. The asymptotic analysis when ε^* vanishes shows that u^0 does not depend on the cell variable y in bases and so depends only on the spatial variable $\widetilde{x}$.

Next, we remark that $u^0(\widetilde{x}, y)$ is a two-scale field, and therefore cannot be directly used as an approximation of the field $u(x)$ in the actual array of cantilevers. So, an inverse two-scale transform is to be applied to u^0. However, we remark that $\widetilde{x} \mapsto u^0(\widetilde{x}, y)$ is continuous, and so u^0 does not belong to the range of the two-scale transform operator and it has no preimage. Hence we introduce an approximated inverse of the two-scale transform, $v(\widetilde{x}, y) \mapsto \overline{v}(x)$, in the sense that for any sufficiently regular one-scale function $u(x)$ and two-scale function $v(\widetilde{x}, y)$,

$$\overline{\widehat{u}} = u + O(\varepsilon^*) \text{ and } \widehat{\overline{v}} = v + O(\varepsilon^*).$$

It turns out that $\overline{v}(x)$ is a mean over the cell including x centered at x^c with respect to $\widetilde{x} = (x_1, x_2)$ when x belongs to a cantilever $\overline{v}(x) = \langle v(., \epsilon^{-1}(x - x^c))\rangle_{\widetilde{x}}$, and with respect to x_2 when x belongs to a base $\overline{v}(x) = \langle v(., \epsilon^{-1}(x - x^c))\rangle_{x_2}$. In total, we retain $\overline{u}^0$ as an approximation of u in the actual physical system. Note that for the model in dynamics, the deflection $u(t, x)$ is a time-space function. In our analysis we do not introduce a two-scale transform in time, so the time variable t acts as a simple parameter.

4. Model description

Now, we describe the model satisfied by the two-scale approximation $u^0(t, \widetilde{x}, y)$ of $u(t, x)$. Remark that as the deflection u in the Kirchhoff-Love model is independent of x_3, thus u^0 is independent of y_3. For further simplicity, we neglect cantilever torsion effect i.e. the variations of $y_1 \mapsto u^0(t, \widetilde{x}, y)$. Thus, cantilever motion is governed by a classical Euler-Bernoulli beam equation, in the microscopic variable y_2,

$$m^C \partial_{tt} u^0 + r^C \partial^4_{y_2 \ldots y_2} u^0 = f^C$$

with $r^C = \varepsilon^{*4} E^C I^C$, where m^C is a linear mass, E^C the cantilever elastic modulus, I^C the second moment of cantilever section, and f^C a load per unit length in the cantilever. This model represents the motion of an infinite number of cantilevers parameterized by all $\widetilde{x} = (x_1, x_2)$.

Bases are also governed by an Euler-Bernoulli equation, in the macroscopic variable x_1, where part of loads comes from the continuous distributions of cantilever shear forces,

$$m^B \partial_{tt} u^0 + r^B \partial^4_{x_1 \ldots x_1} u^0 = -d^B \partial^3_{y_2 \ldots y_2} u^0 + f^B$$

with $r^B = E^B I^B$, where m^B, E^B, I^B, d^B and f^B are a linear mass, the base elastic modulus, the second moment of section of the base, a cantilever-base coupling coefficient and the load per unit length in the base.

In the model, cantilevers appear as clamped in bases. So at base-cantilever junctions,

$$u^0_{|cantilever} = u^0_{|base} \text{ and } (\partial_{y_2} u^0)_{|cantilever} = 0, \tag{2}$$

because $\partial_{y_2} u^0 = 0$ in bases. Equations of free ends are

$$\partial^2_{y_2 y_2} u^0 = \partial^3_{y_2 y_2 y_2} u^0 = 0, \tag{3}$$

and those of ends equipped with a rigid part (usually a tip in Atomic Force Microscopes) are

$$J^R \partial_{tt} \begin{pmatrix} u^0 \\ \partial_{y_2} u^0 \end{pmatrix} + \varepsilon r^C \begin{pmatrix} -\partial^3_{y_2 y_2 y_2} u^0 \\ \partial^2_{y_2 y_2} u^0 \end{pmatrix} = \begin{pmatrix} f_3^R \\ F_3^R + F_2^R \end{pmatrix}$$

at junctions between elastic parts and rigid parts. Here, J^R is a matrix of moments of the rigid part about the junction-plane, f_3^R is a load in the y_3 direction, F_3^R is a first moment of loads about the junction-plane, and F_2^R the first moment of loads in the y_2 direction about the beam neutral plane. Finally, the base clamping conditions are

$$u^0 = \partial_{x_1} u^0 = 0. \tag{4}$$

The loads f^C, f^B and f^R in the model are asymptotic loads which are generally not defined from the physical problem. In practical computations, they are replaced by the two-scale transforms $\widehat{f^C}$, $\widehat{f^B}$ and $\widehat{f^R}$. To be complete, we mention that rows of cantilevers are discoupled, this is why x_2 plays only the role of a parameter.

5. Structure of eigenmodes

There is an infinite number of eigenvalues λ^A and eigenvectors $\varphi^A(x_1, y_2)$ associated to the model. For convenience, we parameterize them by two independent indices i and j, both varying in the infinite countable set $\mathbb{N}$. The first index i refers to the infinite set of eigenvalues λ_i^B and eigenvectors $\varphi_i^B(x_1)$ of the Euler-Bernoulli beam equation associated to a base. The eigenvalues $(\lambda_i^B)_{i\in\mathbb{N}}$ constitutes a sequence of positive number increasing towards infinity. At each such eigenvalue corresponds another eigenvalue problem associated to cantilevers, which has also a countable infinity of solutions denoted by λ_{ij}^C and $\varphi_{ij}^C(y_2)$. The index i of λ_i^B being fixed, the sequence $(\lambda_{ij}^C)_{j\in\mathbb{N}}$ is a positive sequence increasing towards infinity. In the other side, for fixed j and large λ_i^B, i.e. large i, the sequence $(\lambda_{ij}^C, \varphi_{ij}^C)_{i\in\mathbb{N}}$ converges to an eigenelement of the clamped-free cantilever model. Finally, we have proved that the eigenvalues λ_{ij}^A of the model are proportional to λ_{ij}^C, and that each eigenvector $\varphi_{ij}^A(x_1, y_2)$ is the product of a mode in a base by a mode in a cantilever $\varphi_i^B(x_1)\varphi_{ij}^C(y_2)$.

6. Model validation

We report observations made on eigenmode computations. We consider a one-dimensional silicon array of N cantilevers ($N = 10$, 15 or 20), with base dimensions $500\mu m \times 16.7\mu m \times 10\mu m$, and cantilever dimensions $41.7\mu m \times 12.5\mu m \times 1.25\mu m$, see Figure 2 for the two possible geometries, with or without tips. We have carried out our numerical study on both cases, but we limit

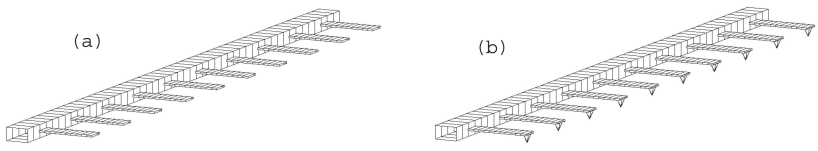

Fig. 2. Cantilever Array with tips (a) and without tips (b)

the following comparisons to cantilevers without tips, because configuration including tips yields comparable results.

We restrict our attention to a finite number n^B of eigenvalues λ_i^B in the base. Computing the eigenvalues λ^A, we observe that they are grouped in bunches of size n^B accumulated around a clamped-free cantilever eigenvalues. A number of other eigenvalues are isolated far from the bunches. It is remarkable that the eigenelements in a same bunch share a same cantilever mode shape, (close to a clamped-free cantilever mode) even if they correspond to different indices j. This is why, these modes will be called *"cantilever modes"*. Isolated eigenelements share also a common cantilever shape, which looks like a first clamped-free cantilever mode shape excepted that the clamped side is shifted far from zero. The induced global mode φ^A is then dominated by base deformations and therefore will be called *"base modes"*. Densities of square root of eigenvalues are reported in the sub-figures 2, 4 and 6[1] of Fig. 3 for $n_B = 10$, 15 and 20 respectively. These figures show three bunches with size n_B and isolated modes that remain unchanged.

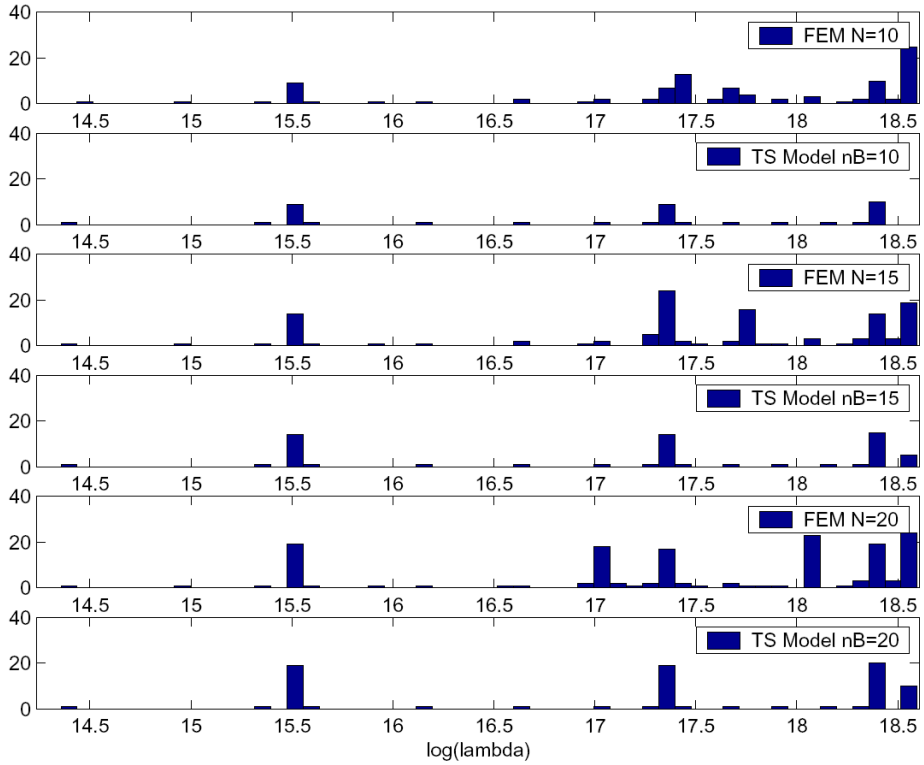

Fig. 3. Eigenmode Density Distributions for Finite Element Model and for the Two-Scale Model

We discuss the comparison with the modal structure of the three-dimensional linear elasticity system for the cantilever array discretized by a standard Finite Element Method. The eigenvalues of the three-dimensional elasticity equations constitute also an increasing positive sequence that accumulate at infinity. As for the two-scale model, its density distribution exhibits a number of concentration points and also some isolated values. Here bunch sizes equal the number N of cantilevers, see sub-figures 1, 3 and 5 in Fig. 3 representing eigenmode distributions for $N = 10$, 15 and 20. Extrapolating this observation shows that when the number of cantilevers increases to infinity bunch size increases proportionally. Since the two-scale model is an approximation in the sense of an infinitely large number of cantilevers, this explains why the two-scale model spectrum exhibit mode concentration with infinite number of elements. This remark provides guidelines for operating mode selection in the two-scale model. In order to determine an approximation of the spectrum for an N-cantilevers array, we suggest to operate a truncation in the mode list so that to retain a simple infinity of eigenvalues $(\lambda_{ij}^A)_{i=1,..,N \text{ and } j\in\mathbb{N}}$. We stress the fact that $N-$eigenvalue

[1]Sub-figures are counted from top to down.

bunches are generally not corresponding to a single column of the truncated matrix λ_{ij}^{A}. This comes from the base mode distribution in this list. When considered in increasing order, base modes are located in consecutive lines of the matrix λ^{A} but not necessary in a same column. We remark that a number of eigenvalues in the Finite Element model spectrum have not their counterpart in the two-scale model spectrum. The missing elements correspond to physical effects not taken into account in the Euler-Bernoulli models for bases and cantilevers.

The next step in the discussion is to compare the eigenmodes and especially those belonging to bunches of eigenvalues. To compare an eigenvector from the two-scale model with an eigenvector of the elasticity system, we use the *Modal Assurance Criterion,* see [5] which is equal to one when the shapes are identical and to zero when they are orthogonal, see Fig. 4 and Fig. 5.

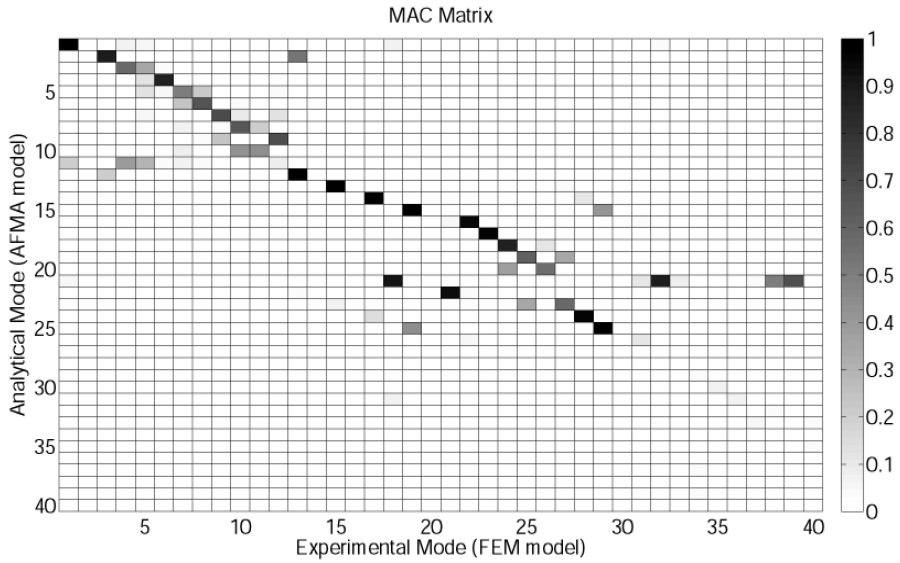

Fig. 4. MAC matrix between two-scale model modes and FEM modes

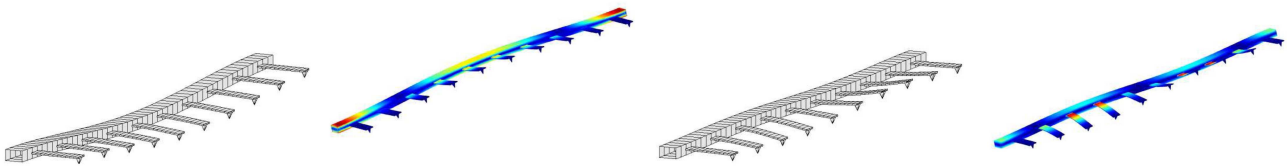

(a) B1-C1 (b) N1 (c) B2-C2 (d) N13

Fig. 5. Two-scale model eigenmode shapes and FEM eigenmode shapes

This test has been applied on transverse displacement only and a further selection has been developed so that to eliminate modes corresponding to physical effects not modeled by the Euler-Bernoulli models. Following this procedure, mode pairing is achieved successfully. In Figure 6(a) paired eigenvalues have been represented and the corresponding relative errors are plotted on Figure 6(b). Note that errors are far from being uniform among eigenvalues. In fact, the main error source resides in a poor precision of the Euler-Bernoulli model for representing base deformations in few particular cases. Indeed, a careful observation of Finite Element modes shows that base torsion is predominant for some modes. This is especially true for the first mode of the first cantilever mode bunch.

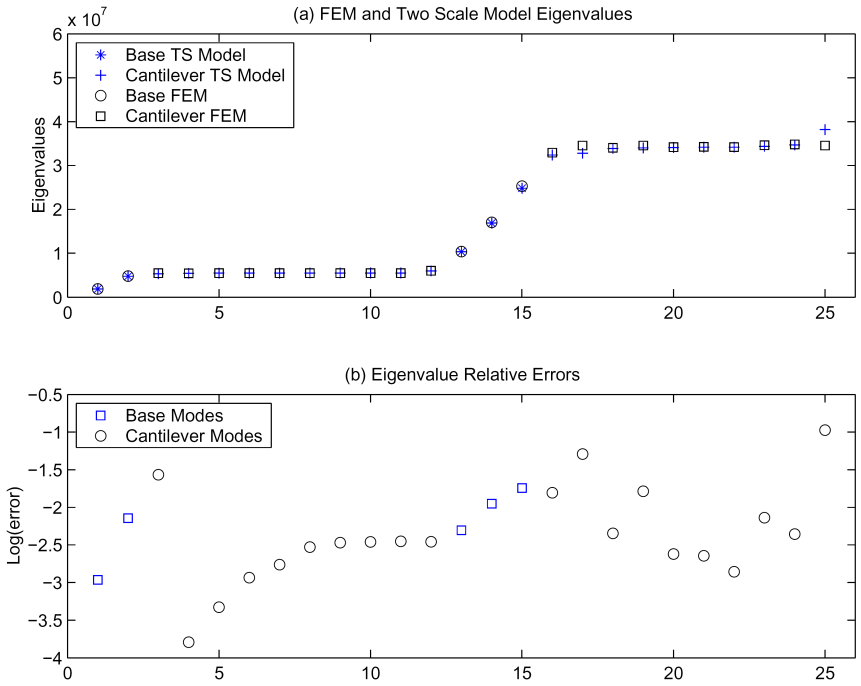

Fig. 6. (a) Superimposed Eigenmode Distributions of the simple Two-Scale Model with the full three-dimensional Finite Element Model (b) Errors in logarithmic scale

7. Model identification

In this section, we report some results related to model identification obtained from a module which is incorporated in the AFM Array simulation tool. The calculations are carried out for an array with ten cantilevers.

7.1 Global Sensitivity Analysis (GSA)

With the GSA we study model sensitivities with respect to parameters by analysing eigenvalues. The model parameters are Young's modulus, Poisson ratio, volume mass, the thicknesses, lengths and widths of base, cantilever and tip. The observations are a list (λ_{ij}^A) of eigenvalues for $i = 1, .., 10$ and $j = 1, 2$, where the index i and j refers to *"base modes"* and *"cantilever modes"* respectively, see Fig. 7.

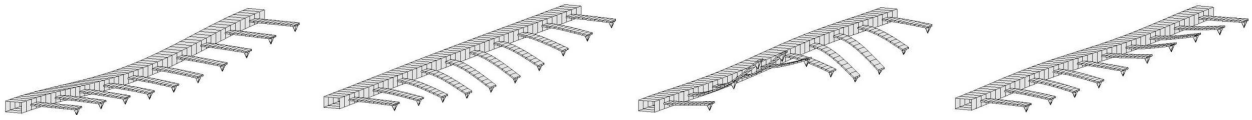

(a) B1-C1 (b) B1-C2 (c) B2-C1 (d) B2-C2

Fig. 7. Model eigenmodes (B=base mode, C=cantilever mode)

For performing the GSA, we consider a sample of parameter vectors issued from the realization of a uniform probability distribution drawn in the intervals bounded by 0.8 and 1.2 times the nominal values. The correlation coefficients matrix between parameters and observations is presented in Fig. 8(a), where parameters are in the horizontal axis and eigenvalues in the vertical axis. We see that the parameters *hB* and *Lbeam* are influential. The number of influent parameters is also indicated by the singular values. Fig. 8(c) shows two significant singular values with respect to the others, which means that only two parameters are influent. Then, the influent parameters are determined using the maximum absolute values of the singular vectors associated with the two

maximal singular values. From Fig. 8(b), we deduce that *Lbeam* and *hB* are the most influent parameters. This result confirms the analysis of the correlation matrix. So, from now, we consider only these two parameters.

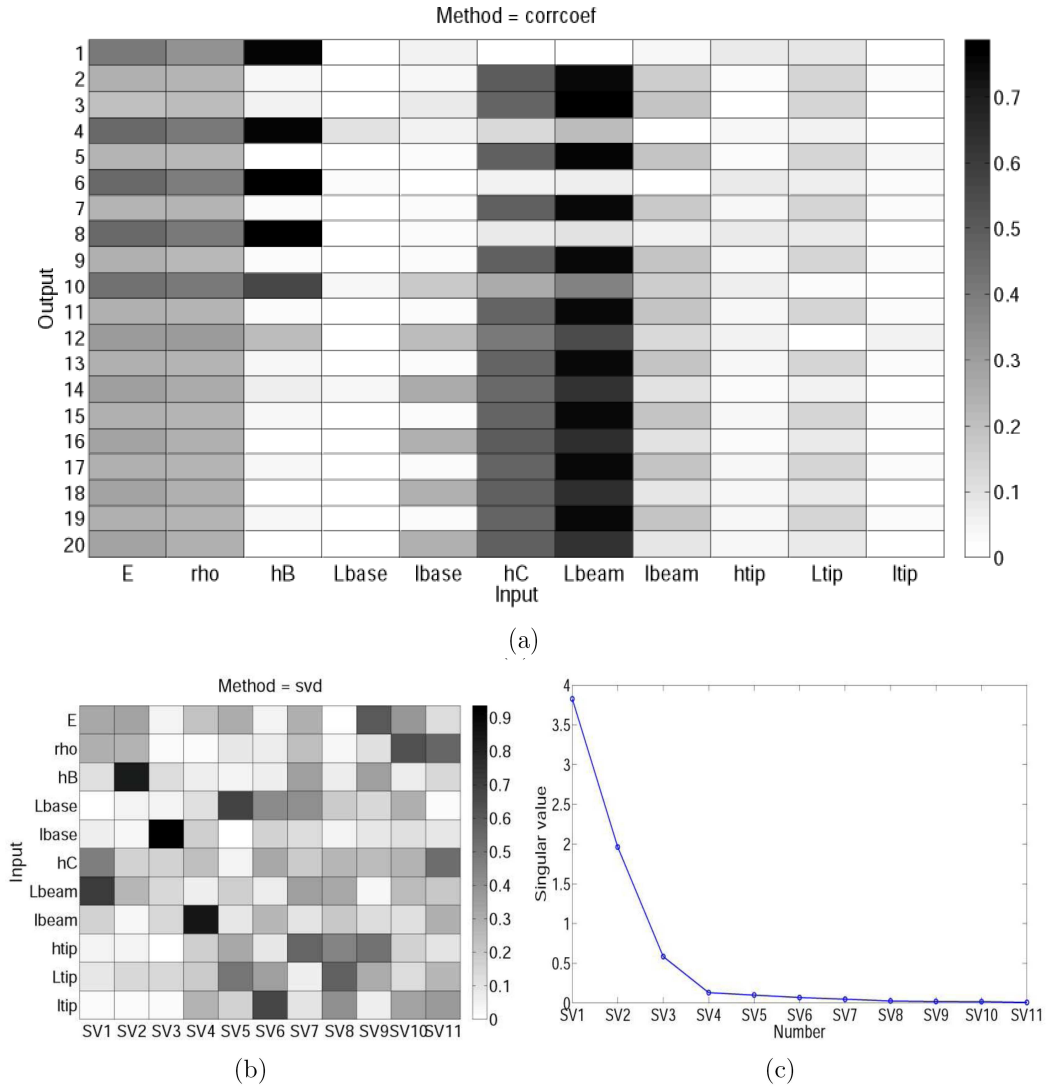

Fig. 8 (a) Correlation coefficient matrix, (b) Singular Value Decomposition matrix, (c) Singular values

7.2 Updating by Sensitivity

Parameter updating through sensitivity is an iterative procedure based on eigenvalue and eigenvector sensitivities with respect to parameters. The algorithm tends to minimize a cost function related to the difference between experimental data (here replaced by outputs of the FEM simulation) and model outputs. We take the GSA into account to restrict the parameter set to *hB* the base thickness and *Lbeam* the cantilever length. We initialize *hB* and *Lbeam* to 1.3 and 0.8 times the nominal values respectively. After 9 iterations, the convergence was reached and the exact value of the reference parameters is returned, see Fig. 9.

7.3 Inverse identification

Generally speaking, an inverse problem consists in identifying the parameters of a physical system from experimental observations. We adopt the Tarantola's formulations [6] for the two parameters *hB*, *Lbeam* to be identified, and for the eigenvalues $(\lambda_{ij}^{A})_{i=1,..,10 \text{ and } j=1,2}$ as observation data. The

Tarantola's formulation combines probability density functions (pdfs) representing the a priori information on the model parameters, the experimental information and the theoretical uncertainty to produce a posteriori pdfs on the model parameters. Here, we assume uniform a priori pdfs for the parameters, Gaussian experimental uncertainties and an exact theory. It is generally difficult to determine directly the *a posteriori* probability distribution. So, it is estimated thanks to a Monte Carlo simulation. As proposed in [7], an algorithm of Metropolis-Hastings [8] is utilized. Two convergence criteria are used, the empirical means and the cumulative sums, see [9]. Here, 500 samples are used for estimating the densities, and the convergence is reached after 124 iterations. The final probability distributions are represented in Fig. 10.

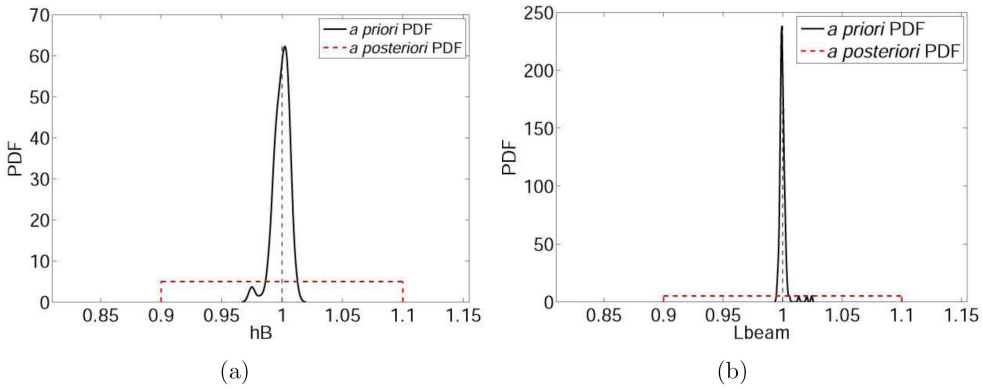

Fig. 10. Identification results for the parameters (a) *hB* (b) *Lbeam*

8. Conclusion

A cantilever array model in dynamic regime have been derived based on a theory of strongly heterogeneous homogenization where the cantilevers play the role of soft parts. We conclude to a globally good agreement with the three-dimensional elasticity model based on eigenvalue and eigenvector comparisons. The model was shown to be sufficiently light to apply successfully usual updating and identification techniques.

References

[1]. M. Despont, J. Brugger, U. Drechsler, U. Durig, W. Haberle, M. Lutwyche, H. Rothuizen, R. Stutz, R. Widmer, G. Binnig, H. Rohrer, and P. Vettiger. Vlsi-nems chip for parallel afm data storage. *Sensors and Actuators, A: Physical*, 80(2):100-107, 2000. Thermomechanical writing; Electrical stability; Time-multiplexed method;.

[2]. M. Napoli, Wenhua Zhang, K. Turner, and B. Bamieh. Characterization of electrostatically coupled microcantilevers. *Journal of Microelectromechanical Systems*, 14(2):295-304, 2005.

[3]. Michel Lenczner and Ralph C. Smith. A two-scale model for an array of afms cantilever in the static case. *Mathematical and Computer Modelling*, 46(5-6):776-805, 2007.

[4] M. Lenczner. A multiscale model for atomic force microscope array mechanical behavior. *Applied Physics Letters*, 90:091908, 2007.

[5] Randall J. Allemang. The modal assurance criterion - twenty years of use and abuse. *S V Sound and Vibration*, 37(8):14-23, 2003.

[6] A. Tarantola. *Inverse Problem Theory and Methods for Model Parameter Estimation*. SIAM, Philadelphia, 2005.

[7] K. Mosegaard and A. Tarantola. *International Handbook of Earthquake and Engineering Seismology (part A)*, chapter Probabilistic Approach to Inverse Problems. Academic Press, 2002.

[8] N. Metropolis, A. W. Rosenbluth, M. N. Rosenbluth, A. H. Teller, and E. Teller. Equation of state calculations by fast computing machines. *Journal of Chemical Physics*, 1(6):1087-1092, 1953.

[9] B. Yu and P. Mykland. Looking at Markov samplers through Cusum path plots: a simple diagnostic idea. *Statistics and Computing*, 8:275-286, 1998.